



ELSEVIER

Fluid Dynamics Research 30 (2002) 379–399

FLUID DYNAMICS
RESEARCH

On drag, Strouhal number and vortex-street structure

Boye Ahlborn^a, Mae L. Seto^b, Bernd R. Noack^{c, *}

^a*Department of Physics, University of British Columbia, 6224 Agricultural Road, Vancouver, British Columbia, Canada V6T 1Z1*

^b*Defence R&D Canada Atlantic (formerly DREA), #9 Grove Street/P.O. Box 1012, Dartmouth, Nova Scotia, Canada B2Y 3Z7*

^c*Hermann-Föttinger-Institut für Strömungsmechanik, Technische Universität Berlin, Straße des 17. Juni 135, D-10623 Berlin, Germany*

Received 11 October 2001; received in revised form 8 March 2002; accepted 23 March 2002

Communicated by W. Schneider

Abstract

A phenomenological model for the vortex-shedding process behind bluff cylindrical bodies is proposed. Relationships between Strouhal frequency St , drag coefficient c_D , Reynolds number Re and geometric wake parameters are obtained from mass conservation, momentum conservation in the transverse direction and energy considerations. For the first time, Roshko's (Technical Report TN 3169, NACA, US Government Printing Office, Washington DC, 1954) experimental discovery of vortex-street similarity behind different cylinders is analytically derived. In addition, the empirically obtained Strouhal-frequency laws of Roshko (Technical Report TN1191, NACA, US Government Printing Office, Washington DC, 1954) and Fey (Phys. fluids A 10 (1998) 1547) are also reproduced. Measurements of St and c_D including their Re dependency for flows around cylinders with circular, square, triangular, semi-circular and other cross sections agree favorably with the proposed model. © 2002 Published by The Japan Society of Fluid Mechanics and Elsevier Science B.V. All rights reserved.

PACS: 47.27.Vf (wakes); 47.32.Cc (vortex dynamics); 47.32.Ff (separated flows)

Keywords: Wake; Drag; Vortex street

1. Introduction

Flows around bluff bodies at a sufficiently large Reynolds number give rise to periodic shedding of vortices with alternating circulation resulting in the familiar von Kármán vortex street. Vortex streets

* Corresponding author. Tel.: +49-30-314-23359, 23472; fax: +49-30-314-21101.

E-mail address: noackbr@pi.tu-berlin.de (B.R. Noack).

Nomenclature

' ∞ '	This subscript refers to high- Re values of the specified quantity
α	non-dimensionalized wavelength (λ/D)
α^*	aspect ratio (λ/D^*)
β	vortex-size parameter (D^*/D)
γ	non-dimensionalized circumferential velocity of the von Kármán vortex (U^*/U)
δ	boundary-layer thickness
κ	proportionality constant in Eq. (7)
λ	wavelength of the vortex street
ν	kinematic viscosity of the fluid
ρ	density of the fluid
θ	wake-deflection angle (see Eq. (39))
τ_{diss}	vortex dissipation time scale
τ_{prod}	vortex production time scale
A_t	area of the wake river in one wavelength λ
A_e	area of the two vortices in one wavelength λ
B	reduced energy-mode number ($k/2^{11/2}\pi$)
b	width of wake river
c	constant of proportionality in $N = c/\sqrt{Re}$
c_D	drag coefficient
D	diameter of the cylinder
D^*	diameter of the vortex ($2R^*$)
E_c	coherence energy (pressure energy) of both von Kármán vortices in one wavelength λ
E_k	kinetic energy of a single von Kármán vortex
E_r	rotational energy of the wake in one wavelength ($2E_k$)
E_t	translational energy of the wake river in one wavelength
E_λ	total energy of the vortex street in one wavelength ($E_r + E_c + E_t$)
F_D	time-averaged drag force
f	vortex-shedding frequency
k	energy-mode parameter (E_λ/E_r)
k^*	re-scaled energy-mode parameter (βk)
m	constant in the Fey et al. (1998) frequency law
N	vortex-diffusion parameter
R	radius of the cylinder
R^*	radius of the vortex
Re	Reynolds number (DU/ν)
Re^*	non-dimensionalized diffusion parameter ($\pi k N/4$)
Re_c	critical Reynolds number for onset of vortex shedding
St	Strouhal number (fD/U)
St^*	universal Strouhal number (fD^*/U)

T	vortex-shedding period
U	velocity of the oncoming flow
U^\star	circumferential velocity of the von Kármán vortex
u_w	maximum streamwise velocity fluctuation of the wake river
v_w	maximum transverse velocity fluctuation of the wake river
W	width of the cylinder
y_w	centerline of wake river

can be observed behind telephone wires, perceived as Aeolian tones, behind buildings, chimneys and other bluff bodies. Pronounced vortex shedding can also be observed behind bodies which are far from cylindrical, for instance, near the mountains of the Madeira island (Berger and Wille, 1972) and behind tankers after a collision where the tanker oil improves the flow visualization.

The bluff-body wake is utilized in industrial applications. The persistent periodicity of vortex shedding is exploited in a vortex counter as mass-flux meter. The good mixing properties of the vortex street are used in heat exchangers. However, often the drag and periodicity associated with bluff-body wakes are undesirable. Examples include the landing noise due to vortices shedding behind a wing in a high-lift configuration, the hydrodynamic forces on a submarine conning tower, and the potentially hazardous aero-elastic resonances between wakes and elasticity modes of chimneys, bridges and other bluff bodies.

A characteristic feature of the vortex street is its geometric similarity which is nearly independent of the bluff body generating it. This feature of the vortex street suggests that there should be analytical relations between the Reynolds number $Re = UD/\nu$, which describes the boundary condition with the lateral dimension of the obstacle D , the flow velocity U and the fluid viscosity ν and parameters characterizing the flow, including the Strouhal number St , the drag coefficient c_D and the parameters describing the vortex street. There are other structures that also bear little witness to the generating mechanism, namely shock waves in gases and plasma. For these structures, one can give elegant analytical relations linking parameters in the post-shock medium to the equivalent pre-shock quantities and to the shock velocity. A well-known example are the Rankine–Hugoniot conditions for the conservation of mass, momentum and energy augmented by the thermodynamic equation of state. In this study, analogous equations for the vortex-street flow are found. The analysis is accomplished by the use of conservation equations for mass, momentum and mechanical energy, augmented by an equation of state and relations for the accessible modes of the mechanical energy of the fluid.

Roshko (1954b) experimentally investigated laminar and turbulent wakes behind cylinders of different cross sections and observed geometric similarity among all vortex streets. From his data, he derived empirical features of vortex streets that are Reynolds-number independent, and he postulated a ‘universal’ Strouhal number that is related to the wake width. The laminar and turbulent vortex-shedding process is slightly affected by other phenomena as well, e.g. oblique shedding modes, transition modes, Kelvin–Helmholtz instability, boundary-layer effects at the obstacle (see, e.g., the reviews of Berger and Wille 1972; Williamson, 1996; Noack, 1999a, b). However, the main characteristics of the vortex street are not strongly affected by these phenomena.

Development of experimental techniques, like particle-image velocimetry, has provided valuable insight into the shedding processes from small Reynolds numbers to large Reynolds numbers in

the tens of millions (Lin and Rockwell, 1994; Lin et al., 1995; Chyu et al., 1995; Brede et al., 1997). Increasing computational capabilities have helped to reproduce and isolate many experimental findings in the laminar and transitional Reynolds number regime (Karniadakis and Triantafyllou, 1992; Mittal and Balachandar, 1995; Zhang et al., 1995; Henderson, 1996). However, the complexity of the vortex shedding process has eluded an analytical description of the subject. Von Kármán and Rubach (1912) celebrated model describes the vortex street as a staggered periodic chain of vortices with alternating rotational direction and where the spacing is derived from a stability consideration. His model inspired numerous modifications. However, the assumed vorticity distribution, that of point vortices, is far from realistic and the predicted transverse spacing is too large. Von Kármán combined his geometrical model of the vortex street with a momentum consideration to derive a drag relationship. Consequently, numerous drag models have been proposed, mainly focusing on the mean flow (Roshko, 1993). These models have attempted to describe the role of physical and geometric parameters of the mean recirculation zone. However, the Reynolds-number dependency and coherent structures have not been explicitly incorporated. Coherent structures are intimately related to fluctuation amplitudes of drag and lift and also to the mean flow quantities.

In the present study, we pursue Roshko's universal vortex street parameters and von Kármán's concept to derive bluff-body drag from a phenomenological model of the wake kinematics. The model and its implications are outlined in Section 2. The predictions are compared with experimental formulae and data for the Strouhal number and the drag coefficient (Section 3). Finally, the study is summarized and discussed (Section 4).

2. Model

In this Section, a phenomenological model for bluff-body wakes is proposed. In Section 2.1, the main assumptions are outlined. The corresponding constitutive model equations are derived in Section 2.2. Using the model, aspects of the onset of vortex shedding (Section 2.3), the intermediate (Section 2.4) and the high Reynolds number regime (Section 2.5) are described.

2.1. Assumptions

The phenomenological near-wake model describes a cylindrical object which translates with constant speed U through ambient fluid and has lateral dimension D . This model is based on three major experimental and analytical findings related to the geometry of the vortex street, the energy associated with the streamwise motion, and a momentum analysis of the transverse motion.

2.1.1. Vortex-street geometry

The cylindrical object generates a nearly periodic vortex street downstream characterized by a streamwise wavelength λ . The vortex street consists of a meandering river and a staggered array of vortices with alternating vorticity direction (see, for instance, Fig. 3.22, 3.23, 5.16 and 5.19 in Zdravkovich, 1997 or Schlichting and Gersten, 1999). The vortices do not translate much with respect to the ambient fluid. For reasons of simplicity, the vortices are assumed to be Rankine vortices of diameter $D^* = 2R^*$ and circumferential velocity U^* . Fig. 1 illustrates this assumption.

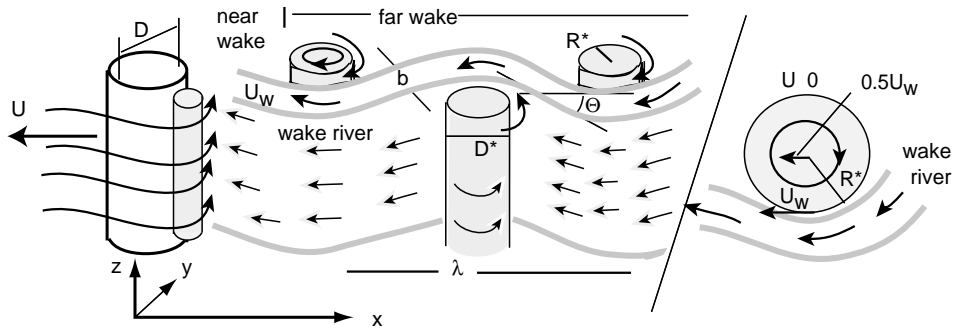


Fig. 1. Principal sketch of the wake generated by a bluff cylindrical object of diameter D and span W . The object travels with constant speed U through ambient fluid.

The described periodic structure is observed in numerous flow visualizations (see, for instance, Ahlborn et al., 1998) and simulations (see, for instance, Zhang et al., 1995). Williamson (1989) measures the velocity of the vortices in the laminar regime. The vortices follow the cylinder with speed $0.15 U$ in the near-wake and lower velocities still further downstream. This small translational vortex velocity is consistent with measurements in the turbulent Reynolds number regime. Thus, the assumption of stationary vortices is roughly consistent with experiment.

The nearly stagnant vortex street is linked to the observed rapid decline of the wake deficit behind the mean recirculation zone which is only approximately one cylinder diameter long (Balachandar et al., 1997). The streamwise decline of the transverse velocity difference is caused by the good initial mixing properties in the vortex formation region near the recirculation zone. Further downstream, the wake river is essentially ‘detached’ from the obstacle and its speed significantly smaller than the speed of the cylinder. The vortices follow the obstacle at an even smaller speed than the wake river due to the displacement towards the ambient fluid. Hence, the assumption of stagnant vortices is applicable behind the vortex formation region and its accuracy improves in the streamwise direction.

2.1.2. Mechanical energy of the wake fluctuation

The cylinder motion through the ambient fluid generates a drag force, F_D , and corresponding ‘towing’ power, $F_D U$. This power is assumed to be completely converted into mechanical wake energy. This assumption is made in finite-wing theory (see, for instance, Panton, 1984) where the trailing edge vortices are related to the wing drag.

The towing power initiates the motion of the full wake: the mainly translational motion of the wake river, the rotation of the vortices, and the pressure energy of the vortices. The latter can be defined by the pressure defect $p - p_\infty$ integrated over the vortex volume, $\int dV(p - p_\infty)$, where p_∞ represents the static pressure of the ambient fluid. The pressure defect holds the spinning vortex together against centrifugal forces and is a measure of the coherence of the vortex. Hence, Ahlborn et al. (1991) call this quantity ‘coherence energy’. While the translational and rotational energy represent two forms of the kinetic energy, the coherence energy may be viewed as potential energy due to the pressure field. This pressure energy may be released in kinetic energy in the spirit of Malkus (1956). This interpretation is corroborated by the Ahlborn et al. (1991) numerical study of

vortex interactions in which the sum of kinetic and coherence energies is found to be approximately conserved, whereupon each form of energy significantly changes with time.

Eventually, the mechanical wake energy converts to thermal energy (heat). We assume that the viscous dissipation per wavelength λ and per shedding period T is small compared to the total energy generated by the towed cylinder during this period. This assumption is plausible for the considered shedding regime, i.e. at Reynolds numbers $Re = UD/\nu \gg 1$, (ν is the fluid kinematic viscosity).

2.1.3. Vorticity production and transverse momentum

In Ahlborn et al. (1998), the vortex-shedding process is analytically investigated with the transverse component of the momentum equation and the vorticity equation. The analysis takes into account the vortex production, convection and dissipation mechanisms and their effects on transverse fluid motion. The following equation for the Strouhal frequency $St = fD/U$ is subsequently derived,

$$St^2 + \frac{4N}{\beta^2 Re} St = \frac{c_D + 1}{2^{3/2} \pi^2 \beta^2}. \quad (1)$$

The first term on the left-hand side (l.h.s.) arises from the near-wake inertia. The second term on the l.h.s. is associated with vorticity diffusion. This term contains the normalized vortex diameter defined as

$$\beta = D^*/D \quad (2)$$

and a dimensionless empirical diffusion parameter N which describes the strength of the vorticity gradient. The right-hand side (r.h.s.) of Eq. (1) is related to vorticity production $(c_D + 1)U^2/2$, where c_D is the drag coefficient. This vorticity production was rigorously derived from the vorticity equation without simplifying assumptions. The term contains the well-known contribution $U^2/2$ from free shear layers (Cottet and Koumoutsakos, 2000) and also incorporates the effect of the pressure field due to form drag. This analysis agrees favorably with experiment in Ahlborn et al. (1998).

2.2. Constitutive model equations

In the following, three constitutive model equations are derived from the assumptions outlined in the previous section. These equations constitute the main part of the model from which most insights of the wake dynamics are obtained in the following sections. Their derivation is based on kinematic considerations and the mass, momentum and energy balance equations of fluid mechanics without utilizing further approximations.

The geometric wake assumption implies that in the bluff body's fixed frame of reference the wavelength λ of the vortex street is the product of the oncoming velocity U and the shedding period $T = 1/f$, or, equivalently, $\lambda f = U$. The relationship can be expressed as a function of the non-dimensionalized wavelength $\alpha = \lambda/D$ and the Strouhal number $St = Df/U$, yielding $\alpha St = 1$. Alternatively, the wavelength–frequency relationship can be expressed in terms of wake-intrinsic properties. Following Roshko (1954b), we introduce the ‘universal’ Strouhal number $St^* = fD^*/U$ and the aspect ratio $\alpha^* = \lambda/D^*$. Thus,

$$\alpha St = \alpha^* St^* = 1. \quad (3)$$

An energy balance yields a second relationship as follows. The energy required to tow the cylinder of spanwise length W through the ambient fluid for one period is $F_D \lambda$. The drag force can be

expressed in terms of the drag coefficient c_D by $F_D = \frac{1}{2} c_D \rho U^2 D W$ and the wavelength by $\lambda = D/St$. Thus,

$$F_D \lambda = \frac{1}{2} c_D \rho U^2 D^2 W / St. \tag{4}$$

The energy contained in one wavelength of the vortex street consists of the rotational kinetic energy E_r of a pair of counter-rotating Rankine vortices, the associated coherence energy E_c (Ahlborn et al., 1991), and the translational kinetic energy E_t of the river, i.e. the total energy is given by $E_\lambda = E_r + E_c + E_t$. The rotational energy of the Rankine vortex E_k is, by definition, the kinetic energy of a solid body with constant density ρ , height W , radius R^* , and circumferential velocity U^* , i.e. $E_k = \frac{\pi}{4} \rho R^{*2} U^{*2} W$. The ratio $\gamma = U^*/U$ between the circumferential velocity of the vortex and the free-stream velocity can be estimated from the phenomenological picture. The velocity difference across the vortex diameter D^* is $2U^*$. Assuming that the vortex has no slip with the two flow regions with velocity 0 and U , the velocity difference $2U^*$ is given by U , or, equivalently

$$\gamma = \frac{U^*}{U} = \frac{1}{2}. \tag{5}$$

Thus, the rotational energy becomes

$$E_r = 2E_k = \frac{\pi}{8} \beta^2 \gamma^2 \rho U^2 D^2 W. \tag{6}$$

For a Rankine vortex, the coherence energy has the same magnitude as the kinetic energy (Ahlborn et al., 1991). The contribution of translational, rotational and coherent energy per unit wavelength is summarized as

$$E_\lambda = \frac{1}{2} \kappa \beta^2 \rho U^2 D^2 W, \tag{7}$$

where the non-dimensional parameter κ has been introduced. The ratio between the total energy and the rotational energy per unit wavelength is

$$k = \frac{E_\lambda}{E_r} = \frac{4}{\pi} \frac{\kappa}{\gamma^2} = \frac{16}{\pi} \kappa. \tag{8}$$

This ratio is called the ‘energy-mode parameter’ in the following.

The energy balance implies that $F_D \lambda = E_\lambda$, or, employing Eqs. (4), (7) and (8),

$$c_D = \frac{\pi}{16} k \beta^2 St. \tag{9}$$

This drag relation can be interpreted as follows. With increasing k , the energy content per period increases assuming the other parameters to remain constant. Thus, the towed bluff body must provide more energy to the fluid which implies an increasing drag coefficient. By a similar reasoning, the drag coefficient grows when the vortex size characterized by β increases. The drag coefficient indicates how much energy is put into the fluid per unit time and $\frac{\pi}{16} k \beta^2$ is the energy released per vortex-shedding period. The Strouhal number is, hence, the conversion factor between both time scales in Eq. (9). Eq. (9) seems to contradict the engineering rule-of-thumb that c_D scales inversely with Strouhal number St . However, for geometrically similar vortex streets, k is a constant but $\beta \propto \lambda$ and $St \propto 1/\lambda$. Hence, Eq. (9) implies $c_D \propto 1/St$ for a class of geometrically similar vortex streets in agreement with engineering experience.

The energy-mode parameter k has a simple geometrical interpretation. The flow is considered in a frame of reference at rest with the fluid. The energies associated with the nearly stationary vortices can be described in terms of their areas $A_c = \frac{1}{2} \pi (D^\star)^2$ by $E_r = E_c = \frac{1}{8} A_c \rho W U^2$. The translational energy is stored in a meandering river of width b and follows the bluff body with its velocity U . The river area per wavelength is $A_t = \lambda b$. The translational energy can be expressed by $E_t = \frac{1}{2} A_t \rho W U^2$. Thus, the energy-mode parameter is a function of the ratio between these two areas,

$$k = \frac{E_t}{E_r} = \frac{E_t + E_r + E_c}{E_r} = \frac{E_t + 2E_r}{E_r} = 2 + 4 \frac{A_t}{A_c}. \quad (10)$$

This relation indicates that the achievable density of rotational vortex street energy is less than the density of translational motion energy.

Eq. (10) may also be interpreted with a thermodynamics analogy. The rotational energy E_r may be associated with the energy of a single degree of freedom in analogy to $kT/2$ (k : Boltzmann factor, T : temperature). Then, the energy-mode parameter k is analogous to the thermodynamic degrees of freedom n . In thermodynamic equilibrium, one would expect a value of $k = 3$, i.e. the same energy in the translational, rotational and coherent mode of energy. In fluid dynamics, there is no reason to expect this equilibrium.

The conservation of momentum (1) is the third constitutive model equation. Elimination of β in Eqs. (1) and (9) yields

$$St \left(c_D + \frac{Re^\star}{Re} \right) = B(c_D + 1), \quad (11)$$

where the ‘reduced energy-mode number’ B and the ‘vorticity-diffusion parameter’ Re^\star have been introduced to emphasize the simple structure of the drag–frequency relation. These parameters are defined by

$$B = \frac{k}{2^{11/2} \pi},$$

$$Re^\star = \frac{\pi k N}{4}.$$

This drag–frequency relation (11) can loosely be interpreted as follows. The r.h.s. is related to vorticity production. The first and second term of the l.h.s. can be related to the vorticity accumulated in the vortices and the vorticity lost by diffusion, respectively. Diffusion reduces the Strouhal frequency since the vorticity needs longer to cumulate to a given size vortex.

The wake flow is characterized by six parameters of which two (c_D , St) depend on the time-dependent force on the bluff body, two (α , β) are related to the vortex-street geometry, and two (N , k) are associated with the energies. These parameters can also be further categorized in terms of streamwise and transverse motions. Table 1 summarizes the independent parameters. The Reynolds number characterizes only the boundary condition and not the property of the vortex-shedding process in the wake. The universal wavelength $\alpha^\star = \alpha/\beta$ and universal Strouhal number $St^\star = \beta St$ can be derived from the set of independent parameters.

Table 1
List of the six flow parameters and their interpretation

Parameters related to streamwise motion	... transverse motion	corresponding equation
... force on object	(1) $c_D = \frac{2F_D}{\rho U^2 D W}$	(2) $St = \frac{Df}{U}$	Conservation of momentum
... vortex street kinematics	(3) $\alpha = \frac{\dot{\lambda}}{D}$	(4) $\beta = \frac{D^*}{D}$	Conservation of mass
... vortex street dynamics	(5) $k = \frac{16}{\pi} \frac{F_D \dot{\lambda}}{\rho U^2 D^2 W}$ Alternatively: $B = \frac{1}{2^{11/2} \pi} k$	(6) N Alternatively: $Re^* = \frac{\pi}{4} kN$	Conservation of energy

In summary, three constitutive model Eqs. (3), (9) and (11) relate the Reynolds number and the six wake flow parameters in Table 1,

$$F_n(Re, c_D, St, \alpha, \beta, k, N) = 0, \quad n = 1, 2, 3. \tag{12}$$

Ideally, there are as many relations as parameters. However, some of these are probably body-specific and hence more complicated. Here one can think of three further relations which would close the system of equations: (1) The dynamics of viscous dissipation in the vortex shear-layer, (2) the mechanism of initial vortex formation near the object, and (3) the distribution of energy between the three mechanical energy modes (translational, rotational, and coherent) in the wake. The first connects Re , N and β . The second links Re , α , β and St , and requires detailed knowledge of the bluff-body shape. The third ties together c_D , Re , St , and N . In the spirit of looking for general relations between the vortex-shedding parameters, we avoid these object-specific relations, and settle for relations containing several parameters.

With six parameters in a system of three equations, only three parameters can generally be expected to be eliminated by Eq. (12), leaving three wake parameters in each formula, e.g. $c_D = c_D(Re, \alpha, \beta, k)$, $St = St(Re, \alpha, \beta, k)$, etc. In the following sections it turns out that there is more structure and beauty in the constitutive model equations. This structure can be exploited to remove more adjustable parameters as will be shown next.

2.3. Onset of vortex shedding

The mechanism for the onset of vortex shedding can be explained by vorticity production and dissipation considerations. Vortex shedding can be expected to occur if the dissipation time scale τ_{diss} for vortex decay is larger than its production time τ_{prod} . Two vortices are produced per shedding period $T = 1/f = D/St U$, i.e. the production time is given by

$$\tau_{prod} = \frac{T}{2} = \frac{D}{2St U}. \tag{13}$$

In order to estimate the dissipation time, the von Kármán vortex is modeled by an Oseen vortex. Its circumferential velocity distribution is given by $u_{\text{Oseen}} = (\Gamma/2\pi r)[1 - \exp(-r^2/4vt)]$, where Γ represents the circulation and r the radial distance from the vortex center (see, for instance, Panton, 1984). The e-folding time scale with the vortex core radius R^\star reads (see, for instance, Ahlborn et al., 1985),

$$\tau_{\text{diss}} = \frac{R^{\star 2}}{16\nu} = \frac{\beta^2 D^2}{64\nu}, \quad (14)$$

using $R^\star = D^\star/2 = \beta D/2$. Vortex shedding occurs if the dissipation time is larger than the production time, i.e. $\tau_{\text{diss}} \geq \tau_{\text{prod}}$. Hence, $\tau_{\text{diss}} = \tau_{\text{prod}}$ and Eqs. (13) and (14) define the onset Reynolds number to be $Re_c = 32/\beta^2 St$. The Strouhal number can be eliminated with the energy equation (9),

$$Re_c = \frac{2\pi k}{c_D}. \quad (15)$$

According to Eq. (15), the critical Reynolds number increases with decreasing drag coefficient, i.e. with more streamlined obstacles. The onset is also delayed by an increasing energy-mode parameter k , i.e. decreasing amount of kinetic energy in rotational form. Both trends are physically plausible.

For the flow around a circular cylinder, we obtain $Re_c = 46$ using typical values, $c_D = 1.5$ at low Reynolds numbers and $k = 11$ of Section 3.2. This estimate is in good agreement with the value of $Re_c = 46$ predicted by linear stability theory for the circular cylinder (Jackson, 1987; Zebib, 1987; Noack and Eckelmann, 1994).

2.4. Intermediate Reynolds number regime

In the intermediate Reynolds number regime, where viscosity effects still play a role, Eqs. (3), (9) and (11) are applicable. From this set of equations, one can derive relations between c_D , α and β as function of St , Re , Re^\star and B , namely

$$St = B \frac{c_D + 1}{c_D + Re^\star/Re}, \quad (16)$$

$$c_D = \frac{B - St Re^\star/Re}{St - B}, \quad (17)$$

$$\alpha = \frac{1}{St} = \frac{c_D + Re^\star/Re}{B(c_D + 1)}, \quad (18)$$

$$\beta = \frac{1}{2^{3/4}\pi St} \sqrt{\frac{c_D(c_D + 1)}{c_D + Re^\star/Re}}. \quad (19)$$

Relation (16) predicts that the Strouhal number should increase with Reynolds number and should converge asymptotically to a finite value, as observed in experiments. The drag formula (17) has an interesting, non-trivial implication. The drag coefficient can only be finite and positive for all Re if $B < St < BRe/Re^\star$. In other words, the model imposes a lower and upper bound on the Strouhal

number. In addition, the inequality can only be fulfilled at $Re > Re^*$, i.e. Re^* can be considered as a lower bound for the critical Reynolds number for the onset of vortex shedding. The following analysis of experimental data in Section 3 confirms this interpretation. Eq. (18) brings out the inverse proportionality between shedding frequency and wavelength. This equation is, of course, equivalent to the Strouhal equation (16) appreciating the inverse proportionality between shedding frequency and wavelength (3). The vortex-size equation (19) indicates that diffusion at low Re values increases the vortex size.

2.5. High Reynolds number regime

At high Reynolds numbers, the wake parameters asymptotically approach values which can be inferred from Eqs. (16)–(19) and are denoted by the subscript ‘∞’:

$$St_\infty = B \frac{c_{D,\infty} + 1}{c_{D,\infty}}, \tag{20}$$

$$c_{D\infty} = \frac{B}{St_\infty - B}, \tag{21}$$

$$\alpha_\infty = \frac{c_{D,\infty}}{B(c_{D,\infty} + 1)}. \tag{22}$$

The vortex-size parameter β is intimately linked to the universal wake parameters,

$$St_\infty^* = \beta_\infty St_\infty = \frac{D_\infty^*}{\lambda_\infty} = \frac{1}{2^{3/4}\pi} \sqrt{c_{D,\infty} + 1}, \tag{23}$$

$$\alpha_\infty^* = \frac{\lambda_\infty}{D_\infty^*} = \frac{2^{3/4}\pi}{\sqrt{c_{D,\infty} + 1}}. \tag{24}$$

Eq. (20) reveals that a large drag coefficient is associated with a small variation in the Strouhal number in dependency of Re , since $B < St < St_\infty$. The wake dynamics of a bluff body is dominated by pressure fields and less by viscous diffusion. For instance, the flame-holder with a triangular cross section or a plate has a large drag coefficient and its shedding frequency depends only weakly on the Reynolds number. In contrast, diffusion and boundary-layer effects play a larger role for the laminar wake of more streamlined cylinders with small c_D .

The proportionality between the Strouhal number St_∞^* and the reduced energy-mode number B , expressed by Eq. (20), can be interpreted in geometric terms. A small B indicates that a large portion of the wake energy is concentrated in rotational energy and correspondingly larger wake vortices. Larger vortices imply a longer wavelength and hence a smaller Strouhal frequency. Eq. (23) is the most significant result to this point. The universal aspect ratio $St_\infty^* = \beta_\infty St_\infty = D_\infty^*/\lambda_\infty$ of the vortex street is independent of the energy-mode parameter k , and only a function of $c_{D,\infty}$. This implies that the distribution of energy between rotation, coherence energy, and translational river energy is stable. The vortex street retains no features of the bluff-body geometry that generated it. Therefore, one finds the same wake structure for all bluff bodies that have the same drag coefficient. Eqs. (21) and (22) confirm our interpretation from the discussed Strouhal- and vortex-size equations (18) and (19).

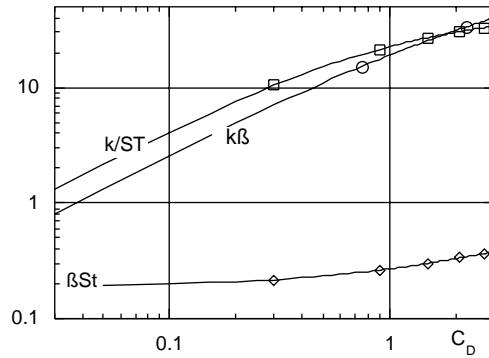


Fig. 2. Three invariants of vortex streets at large Reynolds numbers in dependency of the drag coefficient, βSt (\diamond), $k\beta$ (\circ), and k/St (\square).

Three invariants, which depend only on $c_{D,\infty}$, can be constructed from Eq. (9). This equation can be rewritten as $c_D = \frac{\pi}{16} k^* St^* = \frac{\pi}{16} (k/St) (St^*)^2$ with the universal Strouhal number $St^* = \beta St$ and the re-scaled energy-mode parameter $k^* = \beta k$. Since the l.h.s. and St^* depend only on c_D at large Re , k^* and k/St similarly depend only on c_D at large Re . These invariants are displayed in Fig. 2. Apparently, the drag coefficient is the most important order parameter of turbulent vortex streets.

As an example, the universal Strouhal number is calculated for the circular cylinder with $c_D = 1.1$. We obtain $St_\infty^* = 0.274$. Roshko (1954b) measures a similar universal Strouhal number of 0.28 for a large class of cylindrical cross sections. The small Strouhal number variations for the cylinders studied can be attributed to the fact that Roshko's bluff bodies have $c_D \approx 1$ and that St_∞^* in Eq. (23) depends only weakly on c_D . The universal aspect ratio is $St_\infty \beta_\infty = 0.27$.

3. Analysis of experimental data

In this section, experimental values of drag, Strouhal number and Reynolds number from the literature are combined with the model relations in order to look at known functional relations and to extract new insight into the structure of vortex streets. In Section 3.1 the model is shown to correctly predict empirical frequency laws. In Section 3.2, the vortex shedding behind a circular cylinder at high Reynolds numbers is discussed. In particular, the change of the vortex-street geometry throughout the drag crisis is analyzed. In Section 3.3, the vortex-street geometry is studied for various cylindrical objects with circular and other cross sections.

3.1. Frequency laws

In Eq. (16), the Strouhal number is expressed as a function of B , c_D , Re^* , and Re . We assume that the first three quantities depend weakly on Re . At large Re , the denominator of Eq. (16) can be expanded to first order in $1/Re$, thus yielding

$$St = St_\infty \left(1 - \frac{b}{Re} \right), \quad (25)$$

where St_∞ is described by Eq. (20) and $b = Re^\star/c_D$. This frequency law has the form of Roshko's empirical formula for the laminar wake behind a circular cylinder,

$$St = 0.212 \left(1 - \frac{21.2}{Re} \right). \quad (26)$$

Therefore, a rough estimate of Re^\star and k can be obtained:

$$Re^\star = bc_D = 21.2c_D, \quad (27)$$

$$k = 2^{11/2}\pi B = 2^{11/2}\pi St_\infty \frac{c_D}{c_D + 1}. \quad (28)$$

With $c_D = 1.1$ at $Re \sim 100$, Eq. (27) yields $Re^\star = 23$. Thus, Re^\star is a conservative lower bound for the critical Reynolds number $Re_c = 46$ at the onset of vortex shedding, as speculated in Section 2.4. $Re^\star = 23$ coincides with the boundary for the diffusion-dominated regime $Re < 25$ of the cylinder wake. In this regime, no vortex shedding can be excited because the viscous dissipation continuously overwhelms the vorticity production rate. Mathematically this is revealed in the stability spectrum, which has no pronounced complex conjugated eigenvalue pair (Noack and Eckelmann, 1994).

Eq. (28) yields an energy-mode parameter of $k = E_\lambda/E_r = 15.8$ at $St_\infty = 0.212$, $c_D = 1.1$, i.e. only 6% of the total wake energy is stored in rotational form. The analysis reveals that most of the kinetic energy is stored in the translational mode. This energy distribution explains the applicability of quasi-steady flow models for the drag analysis (Roshko, 1993; Balachandar et al., 1997). The dominance of the time-averaged flow in the energy flux as compared to the contribution of turbulent kinetic energy is also observed in the diffuser flow, even in the transitory stall regime (Coller et al., 2000). However, the value for the ratio should not be taken too literally since the formula for rotational energy is based on a crude simplification. In particular, the vortex edge velocity was assumed to be $U^\star = U/2$. In fact, if the circumferential edge velocity was smaller than $U/2$, the energy balance which relates to the measured c_D can still be satisfied if $k = E_\lambda/E_r$ is larger than 3.

Fey et al. (1998) propose another frequency law,

$$St = St^\star + \frac{m}{\sqrt{Re}}, \quad (29)$$

with different values for St^\star and m in different shedding regimes of the circular cylinder wake. Their empirical formula agrees better with experimental data than Roshko (1954a). It is possible to derive Eq. (29) from our model with a refined assumption. In the derivation of Roshko's law, $Re^\star = \pi k N/4$ is assumed to depend weakly on Re . In Ahlborn et al. (1998), N estimates the non-dimensionalized vorticity gradient at the boundary of the von Kármán vortex. During its creation, the von Kármán vortex rolls up the vorticity of the separating boundary layer of thickness δ . According to laminar boundary-layer theory, this non-dimensional thickness varies inversely with the square-root of the Reynolds number, $\delta/D \propto 1/\sqrt{Re}$. Hence, $N \sim D/\delta \propto \sqrt{Re}$. With $N = c\sqrt{Re}$,

$$\frac{Re^\star}{Re} = \frac{\pi}{4} ck\sqrt{Re}. \quad (30)$$

Substituting Eq. (30) in the Strouhal formula (16) and expanding for small $1/\sqrt{Re}$ yields to the first order

$$St = St_\infty \left(1 - \frac{\pi}{4} \frac{ck}{c_D\sqrt{Re}} \right). \quad (31)$$

This Strouhal-frequency law (31) has the same form as the previously proposed Eq. (29) and the coefficients coincide if

$$St_{\infty} = St^{\star}, \quad n = -\frac{4}{\pi} \frac{mc_D}{k}. \quad (32)$$

In the laminar shedding regime, $46 < Re < 160$, $m \approx -1$ and hence $c = 0.1$. The derivation of Eq. (31) assumes a laminar boundary-layer. However, at boundary-layer transition, i.e. $Re \approx 3 \times 10^5$, the Reynolds-number dependent term in Eq. (31) is small and can be neglected. It should be noted that the subtle changes in the different turbulent shedding regimes (Noack, 1999b; Williamson, 1996) require some modifications of the coefficients St^{\star} , m (Fey et al., 1998) and are not considered in our simple model.

3.2. Wake of the circular cylinder

Schewe (1986) experimentally determined Strouhal numbers and drag coefficients for the circular cylinder over a large Reynolds number range, $20\,000 < Re < 10^7$. This range includes the ‘drag crisis’ regime where Strouhal number and drag coefficient vary greatly. An energy analysis of Schewe’s data reveals the variability of the wake parameters and also shows that the high- Re formulae (20)–(23) are valid since $Re \gg Re^{\star}$. The energy-mode and vortex-size parameters can easily be inferred from Eqs. (28) and (23) omitting the subscript ‘ ∞ ’ for high Reynolds numbers,

$$k = 2^{11/2} \pi \frac{c_D St}{c_D + 1}, \quad (33)$$

$$\beta = \frac{1}{2^{3/4} \pi} \frac{\sqrt{c_D + 1}}{St}. \quad (34)$$

Fig. 3 shows the measured Strouhal number and drag coefficient as well as the energy and vortex-size parameters k and β as a function of the Reynolds number. Evidently, the vortex size changes drastically at the drag crisis. This was expected from Schewe’s flow visualizations. However, the wavelength also decreases so that the aspect ratio βSt is maintained. Also, the energetics of the wake seems to be less affected by the drag crisis since k is practically unchanged at the equilibrium value 11, and only drops slightly at $Re = 3 \times 10^6$ where the drag increases again. This implies that even at high Reynolds numbers most of the energy resides in the wake river and the eddies represent only a minor energy contribution. Since $k \approx 11$, one can solve Eq. (33) for St to get a simple relation between Strouhal number and drag coefficient:

$$St \approx 0.077 \frac{C_D + 1}{C_D}. \quad (35)$$

Similarly, an approximation for the vortex-size parameter can be obtained from Eqs. (34) and (35),

$$\beta \approx 1.2 \frac{C_D}{\sqrt{C_D + 1}}. \quad (36)$$

While k is nearly constant, the vortex size β grows steadily with C_D . Eqs. (35) and (36) can be combined to obtain the universal Strouhal number

$$St^{\star} = \beta St \approx 0.92 \sqrt{C_D + 1}. \quad (37)$$

Formulae (35)–(37) derived from the Reynolds-number dependent data of a bluff body will be compared with cylinders of different cross sections in Section 3.3.

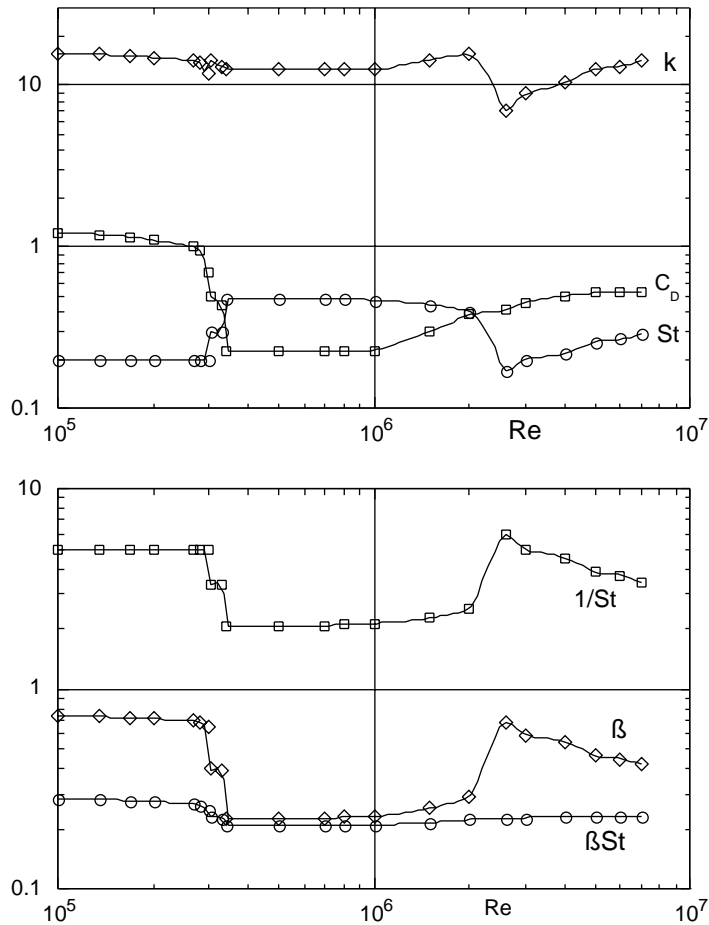


Fig. 3. Analysis of Schewe's data in dependency of the Reynolds number. In the upper figure, the Strouhal data St is denoted by an open circle (\circ), the drag coefficient c_D by an open square (\square) and the energy-mode parameter k obtained from Eq. (33) by a diamond (\diamond). In the lower figure, the universal Strouhal number $St^* = \beta St$ (\circ), the aspect ratio $1/\alpha = \lambda/D = 1/St$ (\square), and the vortex-size parameter β derived from Eq. (34) (\diamond) are shown.

The parameter k derived here from experimental Strouhal numbers and drag coefficients, can alternatively be displayed as functions of the eddy size β (see Fig. 4). This presentation emphasizes the fact that the drag coefficient increases with eddy size, and that the energy fraction k in the wake is practically independent of eddy size. A bifurcation may be occurring for large eddies ($\beta > 0.65$), where both k and c_D become double valued. There is no current explanation for this phenomenon.

3.3. Wake of cylinders with various cross sections

The formalism developed in this study permits to investigate the vortex streets of bluff bodies where measured drag coefficients and Strouhal numbers exist. The analysis can be carried out analytically by the use of Eqs. (33) and (34) or graphically. For the graphical analysis, a parameter net of curves of equal k - and β -values is drawn into a St - c_D -plane, Fig. 5. An iso- k -curve is

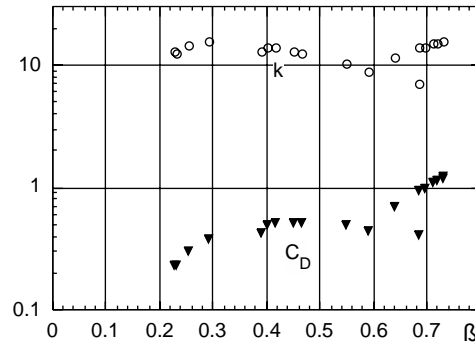


Fig. 4. Energy-mode parameter k (\circ) and drag coefficient c_D (\blacktriangledown) as a function of the vortex-size parameter β from the data of Fig. 3.

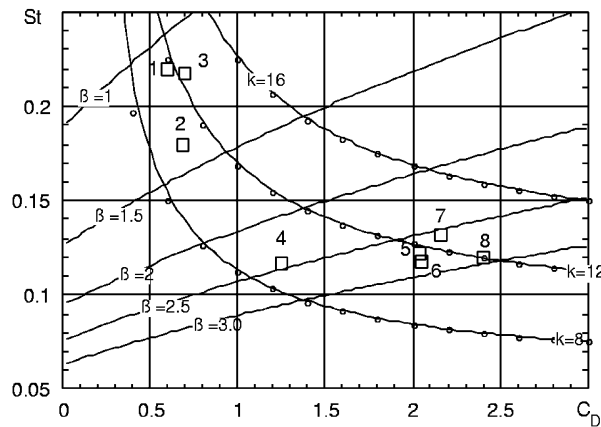


Fig. 5. Strouhal number St as function of the drag coefficient c_D for various body shapes. The figure displays the data (St, c_D) in an iso- k and iso- β net. The numbered open squares indicate the kind of the cross section. The numbers refer to following data: (1) Store belt bridge (Schewe and Larsen, 1998), $Re = 5 \times 10^4$; (2) Store belt bridge (Schewe and Larsen, 1998), $Re = 2 \times 10^6$; (3) Circular cylinder (Norberg, 1993), $Re = 13,000$; (4) Takoma narrows (Schewe and Larsen, 1998), $Re = 4.2 \times 10^5 - 8 \times 10^5$; (5), (7), (8) Square cylinder (Vickery, 1966); $Re = 176,000$; (6) Square cylinder (Norberg, 1993); (8) Circular cylinder (Seto, 1990; Seto et al., 1992) at $Re = 9300$.

obtained by solving Eq. (33) for St and inserting, for instance, $k = 12$. Then, $St(c_D, k = 12)$ is plotted, which yields the middle curve of the k -family in Fig. 5. The curves of the β -family are similarly obtained by solving Eq. (34) for St and calculating $St(c_D)$ at various fixed values of β . Experimental data points $St(c_D)$ for various cylindrical bodies are also shown in Fig. 5. By interpolating between the k - and β -curves, one can directly read off the energy-mode parameter k with the vortex-size parameter β . Note that the Strouhal frequency St decreases with increasing β assuming that the other parameters remain constant. Since the assumed speed of propagation U of the vortex street is fixed, the shedding is inversely proportional to the size of the vortex street as characterized by the vortex-size parameter β . At a given shedding frequency, the drag coefficient is seen to increase with the energy-mode parameter k . This parameter characterizes the energy content per unit wavelength which the drag force has to produce.

Table 2

Experimental data and derived quantities for various cross sections. The data sets are sorted by increasing drag coefficient. We use data of Schewe and Larsen (1998) for the store belt bridge and square cylinder at $Re = 10^5$, of Schewe (1984) for the Tacoma bridge and inclined square cylinder, of Seto (1990) for the circular cylinder, of Norberg (1993) for the square cylinder at $Re = 13\,000$, and of Lee (1975) for the square cylinder at $Re = 176\,000$

Source	Re	c_D	St	β	k	βSt	$\tan \theta$	θ
Store belt bridge	2×10^6	0.600	0.220	0.915	11.7	0.201	0.632	32.3°
Store belt bridge	50 000	0.680	0.180	1.15	10.4	0.206	0.648	32.9°
Circular cylinder	4500	0.700	0.217	0.956	12.7	0.208	0.652	33.1°
Tacoma bridge	6×10^5	1.25	0.117	2.04	9.24	0.239	0.750	36.9°
Square cylinder	1.76×10^5	2.04	0.122	2.70	11.6	0.330	1.04	46.0°
Square cylinder	10^5	2.05	0.118	2.36	11.3	0.278	0.873	41.2°
Square cylinder	13 000	0.216	0.132	2.14	12.8	0.283	0.889	41.6°
Inclined square cylinder	6×10^5	2.40	0.120	2.45	12.0	0.293	0.922	42.7°

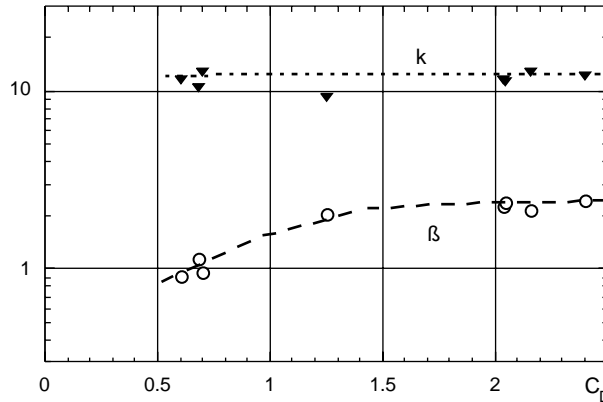


Fig. 6. Vortex-size parameter β (\circ) and energy-mode parameter k (\blacktriangledown) as function of the drag coefficient c_D for the experimental data in Table 2.

All these vortex streets, generated by very different bluff bodies have roughly the same energy-mode parameter $k \approx 11$, which is the same value extracted from Schewe’s data for the circular cylinder over a large range of Reynolds numbers. One can therefore conclude by Eq. (10) that the area ratio of wake river to vortices is $A_t/A_e \approx 11 - 2 = 9$ for all vortex streets at high Reynolds number. This implies that most of the energy is contained in the wake river and not in the vortices. The energy-mode parameter k and other quantities are summarized in Table 2. Employing the approximate formulae (36) and (37) obtained in Section 3.2 for the circular cylinder, we expect that β and $St^* = \beta St$ as reported in Table 2 are only functions of c_D . This expectation is corroborated by a corresponding illustration in Fig. 6.

The universal Strouhal number $St^* = \beta St$ has a useful geometrical interpretation: It characterizes the maximum excursion angle θ of the meandering vortex street, defined in Fig. 1. The wake can be approximated by a wake river which meanders around a staggered array of von Kármán vortices of radius R^* and streamwise wavelength λ (see Sections 2.1 and 2.2). The centerline $y_w(x)$ of the

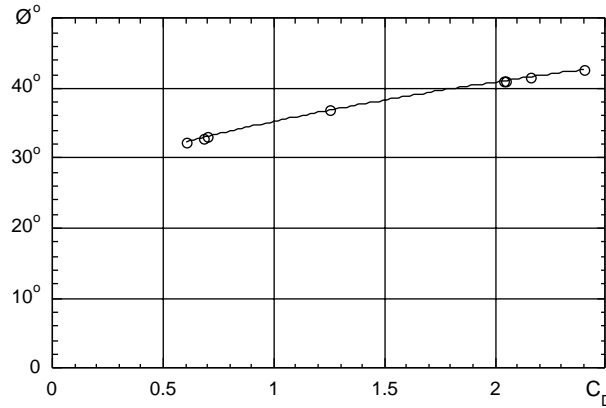


Fig. 7. Maximum deflection angle θ (40) as function of the drag coefficient for the experimental data of Table 2.

wake river can hence be approximated by a sinusoidal wave motion where the amplitude (centerline deformation) scales with the radii of the vortices,

$$y_w = R^* \sin\left(\frac{2\pi x}{\lambda}\right). \tag{38}$$

The maximum slope of this curve dy_w/dx describes the velocity ratio of the transverse wake velocity v_w to the streamwise component u_w with respect to the ambient fluid, i.e.

$$\frac{v_w}{u_w} = \frac{dy_w}{dx} = \frac{2\pi R^*}{\lambda} \cos\left(\frac{2\pi x}{\lambda}\right). \tag{39}$$

The associated maximum deflection angle θ is expressed by $\tan \theta = dy_w/dx_w$. Employing the definition of the Strouhal number, Eqs. (2) and (23), the deflection of the wake river and the amplitude of the velocity ratio (39) can be expressed by

$$\tan \theta = \left(\frac{v_w}{u_w}\right)_{\max} = \left(\frac{dy_w}{dx}\right)_{\max} = \pi \beta St = \pi St^* = \frac{c_D + 1}{2^{3/4}}. \tag{40}$$

The quantity $\tan \theta$ is referred to as the ‘wake-deflection parameter’. This parameter is proportional to the universal Strouhal number St^* which can thus be neatly interpreted as the amplitude of the river deformation. Like the universal Strouhal number, the wake-deflection parameter is only a function of the drag coefficient at high Reynolds numbers. Fig. 7 displays the maximum deflection angle θ as a function of the drag coefficient using the data of Table 2. The change of this angle varies significantly from 32° to 43° . Note also that this angle has a limiting value of $\theta_0 = \arctan 2^{-3/4} = 30.7^\circ$ according to Eq. (40). This limiting angle is approached for bluff bodies when c_D is very small. This finding is corroborated by flow visualizations in the laboratory reference frame (Ahlborn et al., 1998). The corresponding velocity ratio is also in good agreement with numerical data for the wake behind a circular cylinder. The transverse velocity component in the laminar and transitional near-wake is numerically observed to be approximately 60% of the oncoming velocity (Zhang et al., 1994), which corresponds to a velocity ratio of 0.6. Eq. (40) may be used to determine the drag coefficient of a structure if the ratio of the transverse and the longitudinal velocity components u_w and v_w of the wake river are measured.

In summary, the wake geometry is essentially parameterized by two quantities, the energy-mode parameter k and the universal Strouhal number St^* .

4. Conclusions

A phenomenological model is proposed for the formation of the vortices and vortex street downstream of a bluff body. A detailed analysis based on the mass, momentum and energy balance equations yields relationships between the Strouhal number, the drag coefficients and the Reynolds number.

In addition, the onset Reynolds number is predicted and permissible ranges of geometric wake parameters are shown. Thus, well-known trends of the Strouhal number vs. Reynolds number relationships are explained. The discrepancy of the analytical forms of different empirical Strouhal frequency laws are traced back to the vorticity diffusion. Roshko's (1954a) law $St = 0.212(1 - 21.2/Re)$ for the laminar shedding behind a circular cylinder is consistent with a Re -independent diffusion number N in the proposed model. This constancy implies that the diffusion layer of the von Kármán vortex is Reynolds-number independent. However, it is physically more plausible that the diffusion layer scales with the boundary-layer thickness, since the evolving vortex rolls up the shear-layer originating from the separation point. This reasoning leads to a proportionality of the diffusion layer with $1/\sqrt{Re}$ resulting in a frequency law suggested by Fey et al. (1998) for the circular cylinder wake, $St = St^* + m/\sqrt{Re}$. However, for other cylindrical cross sections, it is not a priori evident that the Fey et al. formulae is necessarily superior to Roshko's analytical form. To the best of the authors' knowledge, the model represents the first derivation of an experimentally observed $St-Re$ relationship.

A second important outcome of the model is the Strouhal-drag coefficient relationship. The correlation of St and c_D becomes very evident in the drag crisis regime of the cylinder's wake (Schewe, 1986) where a sudden increase in Strouhal number at $Re = 3 \times 10^5$ is accompanied by a large decrease in drag coefficient. It is empirically known that the Strouhal number varies inversely with the drag coefficient. In the present model, the fine-structure of the $St-c_D$ relationship is elaborated in terms of geometric and energetic wake parameters. Thus, experimental data for St and c_D provide insight into the wake energetics, e.g. how the vortex size is linked to the bluff-body dimensions. Such models may be useful in engineering contexts when only the drag force can be monitored in time for different oncoming velocities. From this drag data, the Strouhal number and thus the $St-c_D$ relationship can be inferred. Thus, wake properties can be indirectly assessed. Furthermore, the universal Strouhal number St^* is shown to be directly proportional to the ratio of transverse to longitudinal velocity components in the wake. This raises the possibility of determining drag coefficients for arbitrarily shaped cylindrical bluff bodies through measurements of the wake velocity components.

Third, Roshko's experimental observation of the universal Strouhal number and the geometric similarity of the vortex street behind cylinders of different cross section is described in the model. Roshko's universal Strouhal number and the vortex-street geometry is shown to depend only weakly on the drag coefficient and is independent of other wake parameters. In addition, the proposed model provides a simple geometric interpretation for the universal Strouhal number in terms of the wake river shape.

Acknowledgements

Stimulating discussions with Martin Brede, Helmut Eckelmann, Uwe Fey, Marcel Lefrançois and Michael König are acknowledged. Helpful suggestions of the referee are appreciated. The research has been partially funded by the Deutsche Forschungsgemeinschaft (No 258/1-1).

References

- Ahlborn, B., Ahlborn, F., Loewen, S., 1985. A model for turbulence based on rate equations. *J. Phys. D* 18, 2127–2141.
- Ahlborn, B., Kevlahan, N., Lefrançois, M., 1991. Coherence energies of turbulent flows. *J. Phys. Essays* 4, 406–416.
- Ahlborn, B., Lefrançois, M., King, H.D., 1998. The clockwork of vortex shedding. *Phys. Essays* 11, 144–154.
- Balachandar, S., Mittal, R., Najjar, F.M., 1997. Properties of the mean recirculation region in the wake of two-dimensional bluff bodies. *J. Fluid Mech.* 351, 167–199.
- Berger, E., Wille, R., 1972. Periodic flow phenomena. *Annu. Rev. Fluid Mech.* 4, 313–340.
- Brede, M., Eckelmann, H., Rockwell, D., 1997. On secondary vortices in the cylinder wake. *Phys. Fluids* 8, 2117–2124.
- Chyu, C., Lin, J.-C., Sheridan, J., Rockwell, D., 1995. Karman vortex formation from a cylinder: role of phase-locked Kelvin–Helmholtz vortices. *Phys. Fluids* 7, 2288–2290.
- Coller, B.D., Noack, B.R., Narayanan, S., Banaszuk, A., Khibnik, A.I., 2000. Reduced-basis model for active separation control in a planar diffuser flow. In: *AIAA Fluids 2000 Conference and Exhibit*, Denver, CO, USA, June 19–22, 2000, also as AIAA-00-2563 paper.
- Cottet, G.H., Koumoutsakos, P., 2000. *Vortex Methods—Theory and Practice*. Cambridge University Press, Cambridge.
- Fey, U., König, M., Eckelmann, H., 1998. A new Strouhal–Reynolds-number relationship for the circular cylinder in the range $47 < Re < 2 \times 10^5$. *Phys. Fluids A* 10, 1547–1549.
- Henderson, R.D., 1996. Nonlinear dynamics and pattern formation in turbulent wake transition. *J. Fluid Mech.* 352, 65–112.
- Jackson, C.P., 1987. A finite-element study of the onset of vortex shedding in flow past variously shaped bodies. *J. Fluid Mech.* 182, 23–45.
- Von Kármán, T., Rubach, H., 1912. Über den Mechanismus des Flüssigkeits- und Luftwiderstandes. *Phys. Z.* XIII, 49–59.
- Karniadakis, G.E., Triantafyllou, G.S., 1992. Three-dimensional dynamics and transition to turbulence in the wake of bluff bodies. *J. Fluid Mech.* 238, 1–30.
- Lee, B.E., 1975. The effect of turbulence on the surface pressure field of a square prism. *J. Fluid Mech.* 69, 263–282.
- Lin, J.-C., Rockwell, D., 1994. Cinematographic system for high-image-density particle image velocimetry. *Exp. Fluids* 7, 110–114.
- Lin, J.-C., Vorobieff, P., Rockwell, D., 1995. Three-dimensional patterns of streamwise vorticity in the turbulent near-wake of a cylinder. *J. Fluids Struct.* 9, 231–234.
- Malkus, W.V.R., 1956. Outline of a theory of turbulent shear flow. *J. Fluid Mech.* 1, 521–539.
- Mittal, R., Balachandar, S., 1995. Effect of three-dimensionality on the lift and drag of nominally two-dimensional cylinders. *Phys. Fluids* 7, 1841–1865.
- Noack, B.R., 1999a. On the flow around a circular cylinder. Part I: laminar and transitional regime. *Z. Angew. Math. Mech.* 79, 223–226.
- Noack, B.R., 1999b. On the flow around a circular cylinder. Part II: turbulent regime. *Z. Angew. Math. Mech.* 79, 227–230.
- Noack, B.R., Eckelmann, H., 1994. A global stability analysis of the steady and periodic cylinder wake. *J. Fluid Mech.* 270, 297–330.
- Norberg, C., 1993. Flow around rectangular cylinders: pressure forces and wake frequencies. *J. Wind Eng. Ind. Aerodyn.* 49, 187–196.
- Panton, R.W., 1984. *Incompressible Flow*. Wiley, New York.
- Roshko, A., 1954a. On the development of turbulent wakes from vortex streets. Technical Report TN 1191, NACA, US Government Printing Office, Washington, DC, 1954.
- Roshko, A., 1954b. On the drag and shedding frequency of two-dimensional bluff bodies. Technical Report TN 3169, NACA, US Government Printing Office, Washington, DC, 1954.
- Roshko, A., 1993. Perspectives on bluff body aerodynamics. *J. Wind Eng. Ind. Aerodyn.* 49, 79–100.

- Schewe, G., 1984. Untersuchung der aerodynamischen Kräfte, die auf stumpfe Profile bei großen Reynolds-Zahlen wirken. Technical Report 84-19, Deutsche Forschungs- und Versuchsanstalt für Luft- und Raumfahrt, Göttingen.
- Schewe, G., 1986. Sensitivity of transition phenomena to small perturbations in flow round a circular cylinder. *J. Fluid Mech.* 172, 33–46.
- Schewe, G., Larsen, A., 1998. Reynolds number effects in the flow around a bluff bridge deck cross section. *J. Wind Eng. Ind. Aerodyn.* 74–76, 829–838.
- Schlichting, H., Gersten, K., 1999. *Boundary-Layer Theory*, 8th Edition. Springer, Berlin.
- Seto, M., 1990. Flow interference effects between two circular cylinders. M.A.Sc. Thesis, Department of Physics and Astronomy, University of British Columbia, Vancouver, BC, Canada.
- Seto, M., Ahlborn, B., Lefrançois, M., 1992. A technique to trigger repeatable vortex wave configurations from bluff bodies. *Phys. Fluids A* 3, 1674–1676.
- Vickery, B.J., 1966. Fluctuating lift and drag on a long cylinder of square cross section in a smooth and turbulent stream. *J. Fluid Mech.* 25, 481–494.
- Williamson, C.H.K., 1989. Oblique and parallel modes of vortex shedding in the wake of a circular cylinder at low Reynolds numbers. *J. Fluid Mech.* 206, 579–627.
- Williamson, C.H.K., 1996. Vortex dynamics in the cylinder wake. *Annu. Rev. Fluid Mech.* 28, 477–539.
- Zdravkovich, M.M., 1997. *Flow Around Circular Cylinders*, Vol. 1: Fundamentals. Oxford University Press, Oxford. etc
- Zebib, A., 1987. Stability of viscous flow past a circular cylinder. *J. Eng. Math.* 21, 155–165.
- Zhang, H.-Q., Noack, B.R., Eckelmann, H., 1994. Numerical computation of the 3-D cylinder wake. Technical Report 3/1994, Max-Planck-Institut für Strömungsforschung, Göttingen.
- Zhang, H.-Q., Fey, U., Noack, B.R., König, M., Eckelmann, H., 1995. On the transition of the cylinder wake. *Phys. Fluids* 7, 779–795.